International Journal of Chronic Obstructive Pulmonary Disease

Dovepress
Taylor & Francis Group

Open Access Full Text Article

ORIGINAL RESEARCH

PGAM5 Modulates Macrophage Polarization, Aggravating Inflammation in COPD via the NF-κB Pathway

Yu Zheng[1,2,*], Yujie Wang[1,*], Jia Li[2], Shaomao Zheng[1], Lipeng Zhang[2], Qiaoyu Li[2], Fayu Ling[3], Qiuli Nie[2], Qiong Feng[1], Jing Wang[1,4], Chengji Jin[1]

[1]Department of Respiratory Medicine, The second Affiliated Hospital, Hainan Medical University, Haikou, 570100, People's Republic of China; [2]The Second School of Clinical Medicine, Hainan Medical University, Haikou, 570100, People's Republic of China; [3]Department of Thoracic Surgery, The second Affiliated Hospital, Hainan Medical University, Haikou, 570100, People's Republic of China; [4]NHC Key Laboratory of Tropical Disease Control, Hainan Medical University, Haikou, 571199, People's Republic of China

*These authors contributed equally to this work

Correspondence: Jing Wang, Email tlfwj@163.com; Chengji Jin, Email Jinchengji3432809@163.com

Background: Chronic obstructive pulmonary disease (COPD) has emerged as a very consequential issue threatening human life and health; therefore, research on its pathogenesis is urgently needed. A prior investigation discovered a significant elevation in the phosphoglycerate mutase 5 (PGAM5) expression in the lung tissue of COPD smoking patients. This rise in expression is closely associated with COPD severity. Nevertheless, the precise molecular processes by which PGAM5 influences the COPD initiation and advancement remain unknown.

Materials and Methods: A COPD model was created using murine alveolar macrophages (MH-S). Flow cytometry, enzyme-linked immunosorbent assay, Western blotting, and other methods were used to detect macrophage polarization, inflammatory factor secretion levels, and changes in PGAM5 and the nuclear factor-κB (NF-κB) pathway.

Results: PGAM5 stimulated macrophage M1 polarization and secretion of the proinflammatory factors interleukin-1β (IL-1β) and tumor necrosis factor-alpha (TNF-α). PGAM5 bound and activated apoptotic signaling-regulated kinase 1 (ASK1), further activating the NF-κB pathway. These implications were reversed when PGAM5 expression was silenced.

Conclusion: PGAM5 can cause an increase in p-ASK1^{T838}, trigger the NF-κB pathway activation, and stimulate the M1 macrophage polarization and production of proinflammatory factors. This finding has significant implications for preventing and treating COPD.

Keywords: COPD, phosphoglycerate mutase 5, macrophage polarization, NF-κB pathway, apoptosis signal-regulating kinase 1

Introduction

In recent years, with the advent of an aging population and the intensification of environmental pollution, the chronic obstructive pulmonary disease (COPD) prevalence has risen, making it the third prevailing common cause of mortality globally.[1] Annually, almost 3 million individuals die from COPD.[2] COPD is a significant concern for public health and socioeconomic challenges.[3] Therefore, the study of the pathologic mechanisms of COPD is vital.

Recent investigations have reported a strong connection between macrophage polarization and COPD development and progression.[4,5] Macrophage polarization refers to the function and morphology of macrophages that can change according to specific microenvironmental signals and create distinct functional phenotypes.[6] The macrophage polarization process involves a series of key signaling pathways and factors. Under the regulation of key factors, the binding of receptors and ligands promotes the activation of multiple signaling pathways, which ultimately leads to the polarization of M0 macrophages toward M1 or M2, inflammation is driven by M1 macrophages, while M2 macrophages have anti–inflammatory and tissue healing-supporting roles, and M1/M2 is constantly in a state of dynamic equilibrium.[7–9] Currently, different scholars have different opinions on the direction of macrophage polarization in the lungs of COPD

Received: 9 October 2024
Accepted: 22 January 2025
Published: 6 March 2025

patients. It has been suggested that M2 macrophages are increased in COPD patients and that M2 macrophage polarization leads to airway remodeling, resulting in the development of COPD.[10,11] However, there are also studies suggesting that increased M1 macrophages in the lungs of COPD patients are involved in the inflammatory response and tissue damage in COPD.[12,13] There is still controversy over which macrophage phenotype is more dominant in the progression of COPD. An in vitro investigation has demonstrated that cigarette smoke extract (CSE) promotes macrophage M1 polarization and proinflammatory cytokines release, encompassing tumor necrosis factor-alpha (TNF-α) and interleukin (IL-1β);[14] Nevertheless, more investigations are necessitated to possess a thorough grasp of the exact process of macrophage polarization. The macrophage polarization was potentially controlled by NF-κB pathway.[15] The transcription factor NF-κB exists in the cytoplasm as heterodimers and/or homodimers, primarily p65 and p50, which contribute to the M1 and M2 macrophage polarization, respectively.[16] Cigarette smoke activates the NF-κB pathway and is strongly linked to COPD occurrence and development.[17,18]

A recent investigation demonstrated that the presence of phosphoglycerate mutase 5 (PGAM5), an unusual mitochondrial threonine/serine phosphatase, is notably raised in the lungs of smokers with COPD contrasted with normal individuals.[19] PGAM5 is an unconventional mitochondrial serine/threonine phosphatase enzyme that involved in several mitochondrial processes, such as the balance of organelles, mitophagy, and cell death.[20] PGAM5 activity may also control the dephosphorylation from Drp1 in macrophages, resulting in stimulating proinflammatory responses in macrophages.[21] Moreover, PGAM5 is a newly discovered controller of inflammasome function that operates autonomously from receptor-interacting serine/threonine-protein kinase 3 (RIPK3) and has been demonstrated to contribute to inflammasome activation and is associated with key inflammatory cytokines that play profound roles in various immune diseases.[22,23] Thus, PGAM5 is closely related to COPD and macrophage polarization.[24] Nevertheless, the current understanding of the molecular regulatory mechanisms is inadequate.

Our study showed that PGAM5 increased the expression of p-ASK1^{T838}, thereby activating apoptotic signaling-regulated kinase 1 (ASK1) and the NF-κB pathway. This could impact the macrophage's polarization and increase the production of inflammatory cytokines, leading to COPD development. Therefore, exploring the contribution of PGAM5 to COPD onset and progression will offer reference and new ideas for innovative prevention and treatment targets for COPD.

Materials and Methods

Cell Purchase and Culture

Murine alveolar macrophages (MH-S) were obtained from Wuhan Pu-nuo-sai Life Technology Co, Ltd, in Wuhan, China. The cells were cultivated in RPMI 1640 medium (CM-0597; Wuhan Pu-nuo-sai Life Technology Co, Ltd (Wuhan, China) enriched with 10% fetal bovine serum (FND500; Excell Bio, Jiangsu, China), 1% penicillin-streptomycin (15070–063, GIBCO, California, USA), and 0.05 mm β-mercaptoethanol. Cell culture conditions were 37 °C and 5% CO_2.

Patients and Specimens

All clinical specimens were acquired from the Second Affiliated Hospital of Hainan Medical University. Smoker control lung tissues (n = 4) were procured from patients who underwent surgery for a benign lung nodule. Tissue specimens were collected from a group of 9 individuals with COPD who underwent lung transplantation and the investigation was accepted with the Ethics Committee of the Second Affiliated Hospital of Hainan Medical University (LW2022178). Patient data is shown in Supplementary Table 1.

CSE Preparation

The tobacco used in the study was a Honghe® Filter tip cigarette with a tar content of 10 mg, nicotine content of 0.7 mg, and carbon monoxide fumes of 12 mg. The cigarette was purchased from Hongyunhonghe Tobacco Co., Ltd (Kunming, China). The smoke from the cigarette was obtained by combusting it in an experimental apparatus with a continuously vacuum-driven airflow. Subsequently, a serum-free medium was introduced to generate a suspension. Prior to adding it to

the cell cultures, a sterile filter with a pore size of 0.22 μm was implemented to filter the gathered CSE.[25] The suspension obtained was considered to be 100% CSE and was diluted with a full culture medium to create a 5% CSE solution for cell culture.

Hematoxylin and Eosin (H&E) Staining

An appropriate amount of lung tissue was collected and placed in 10% neutral formalin, embedded in paraffin, and 4-μm-thick sections were created by a pathological technologist. The sections were processed using a standard histological protocol and stained with H&E.[26]

Immunohistochemical (IHC) Staining

IHC staining was conducted using conventional techniques. The paraffin-embedded tissues were sectioned into 4 μm sections. The tissue pieces were soaked in xylene to remove the wax and then washed with different concentrations of alcohol to restore their moisture. They were then submerged in boiling 0.01 M citric acid buffer (pH 6.0) in a pressure cooker to repair antigens, which was sealed and brought to full pressure for 10 min. The sections were treated for 10 min at ambient temperature with a 3% solution of H_2O_2 for blocking in order to remove any endogenous peroxidases. The specimens were thereafter placed in an incubator at 4 °C overnight, together with the primary antibodies (ABs): mouse anti-CD86 (1:200, ab270719; Abcam, Cambridge, UK), rabbit anti-Akt1 (1:200, ab126534; Abcam, Cambridge, UK), mouse CD206 monoclonal AB (1:50, 60143-I-Ig; Proteintech Group, Wuhan, China), mouse CD68 monoclonal AB (1:100, 66,231-2-Ig; Proteintech Group, Wuhan, China), and rabbit NGAL polyclonal AB (1:100, PA5-79589; Thermo Fisher Scientific, MA, USA). Subsequently, they were incubated with a secondary AB that was coupled to horseradish peroxidase (HRP). The sections were then treated with a developing solution and then stained with hematoxylin as a counterstain. The color was fixed using acidic alcohol and then dried. The tissue slices were observed with a Nikon biological microscope (Nikon UK Ltd, Kingston upon Thames, UK). The IHC pictures were examined with Image-Pro Plus 6.0, and the positivity rate was calculated after quantitative processing (integral optical density (sum)/area (sum)).

Cell Transfection and Small Interfering RNA (siRNA) Knockdown

The conditions for the highest transfection efficiency were determined to be 0.1μM siRNA and 48 h after transfection and were chosen for subsequent siRNA experiments. MH-S cells were collected, counted, and resuspended in a complete medium. The cellular density was calibrated to 1×10^5 cells/mL, and 2 mL of the cellular suspension was introduced into each well of 6-well plates. The cells were allocated into control, siRNA-NC, siRNA-PGAM5-257, siRNA-PGAM5-630, and siRNA-PGAM5-713. The control group contained no siRNA at the time of transfection. All siRNAs were purchased from Gempharmatech (Jiangsu, China). After transfection of the four different siRNA plasmids into MH-S cells, changes in PGAM5 expression were detected using reverse transcription quantitative-PCR. siRNA-PGAM5-257, which most efficiently suppressed PGAM5, was selected for the follow-up experiments. Knockdown efficiency was ascertained 48 h following transfection using Western blotting. The detailed methodology used for siRNA screening is shown in Supplementary Figure 1.

Flow Cytometry

MH-S cells were collected, and different groups of interventions were performed. The cells were labeled with the fluorescent-conjugated ABs CD86-FITC (MultiSciences, Zhejiang, China) and CD206-PE-Cyanine7 (eBioscience, California, USA) and incubated at 4 °C for 15 min in the absence of light. The supernatant was eliminated, the cells were rinsed once, 500 μL of phosphate-buffered saline (PBS) was introduced, and the mixture was vigorously mixed. The levels of CD86 and CD206 expression were measured using a FACS flow cytometer (URIT Medical Electronics Co, Ltd, Guilin, China). Flow cytometry gates were determined by Fluorescence minus one (FMO) controls. FMO control tubes were prepared, add CD206 antibody to CD86 FMO control tube, add CD86 antibody to CD206 FMO control tube, they were detected by flow cytometry. Finally, determine fluorescence dispersion and set precise gates based on the fluorescence signals of FMO control samples and negative control samples.

Enzyme-Linked Immunosorbent Assay (ELISA)

The TNF-α, IL-1β/10, and transforming growth factor-beta (TGF-β) levels in the culture supernatant were quantified using an ELISA test kit (MultiSciences, Zhejiang, China) and adjusted based on standard curves, following the manufacturer recommendations.

Western Blotting

Standard protocols were used for Western blot analysis. In summary, MH-S cells were disrupted with RIPA lysis buffer, and a suitable quantity of 5 x sodium dodecyl-sulfate polyacrylamide gel electrophoresis (SDS-PAGE) loading buffer was introduced containing β-sulfhydryl ethanol was heated in boiling water at 100 °C for 5 min to completely degrade the protein and added. Upon separation, the proteins were electrotransferred onto polyvinylidene difluoride (PVDF) membranes. The membranes were obstructed with 5% skim milk for 1 h at ambient temperature and afterward incubated overnight at 4 °C with the diluted primary ABs listed below: anti-mouse PGAM5 AB (A-3) (1:1000, sc-515880; Santa Cruz Biotechnology, Dallas, TX, USA), phospho-ASK1 (Ser1029) AB (1:1000, AF3549; Affinity Biosciences, OH, USA), rabbit-anti-ASK1 (pT838) polyclonal AB (1:1000, abs149098; Absin, Shanghai, China), recombinant anti-NF-κB p65 (phospho S536) AB [EP2294Y] (1:800, ab76302; Abcam, Cambridge, UK), and recombinant anti-NF-κB p65 AB [E379] (1:800, ab32536; Abcam, Cambridge, UK). Beta-actin AB (1:1000, 100166-MM10; Sino Biological Inc, Beijing, China) was implemented as the loading control. Next, appropriately diluted secondary ABS, goat anti-rabbit IgG H&L (HRP) (1:5000, ab205718; Abcam, Cambridge, UK), and goat anti-mouse IgG H&L (HRP) (1:5000, ab205719; Abcam, Cambridge, UK), were introduced and incubated at ambient temperature for 1 h. Subsequent to the washing step with Tris-buffered saline with 0.1% Tween® 20 detergent (TBS-T), the immunoreactive bands were visualized using a Chemiluminescence Imaging System (Chemiscope 3000; Shanghai Qinxiang Scientific Instrument Co, Ltd, Shanghai, China).

Co-Immunoprecipitation (Co-IP)

Co-IP was performed with an immunoprecipitation kit (ab206996; Abcam, Cambridge, UK). MH-S cells (1×10^6 cells/mL) overexpressing PGAM5 were collected. The cells were chilled to 4 °C and incubated for 30 min. After that, they were centrifugated at a force of 14,000 ×g for 10 minutes at 4 °C with an ice-cold lysis buffer. The supernatants were obtained as whole-cell lysates. The supernatants were then divided into three groups: the cell lysate was implemented as the Input group, an experimental group (PGAM5 flag IP) with FLAG AB (1:30, ab205606; Abcam, Cambridge, UK), and an IgG control group (IgG IP) with IgG ABs (1:100, ab172730; Abcam, Cambridge, UK). The ABs were introduced and incubated overnight at 4 °C. The Protein A/G was rinsed two times with a wash buffer. The mixture was centrifuged with 2000 ×g for an interval of 2 min. The resulting beads were then gathered and rinsed three times with a wash buffer. The beads were immersed in 2 × SDS-PAGE loading buffer and heated for 5 min. They were then centrifugated at 14,000 ×g for 1 min at a temperature of 4 °C. SDS-PAGE was implemented to separate the proteins present in the collected supernatants. The proteins that were separated were deposited electrically onto PVDF membranes. The membranes were obstructed with 5% skim milk for 1 h at ambient temperature and subsequently incubated with diluted primary ABs overnight at 4 °C: anti-mouse PGAM5 AB (A-3) (1:1000, sc-515880; Santa Cruz Biotechnology, Dallas, Texas, USA) and recombinant anti-ASK1 AB [EP553Y] (1:800, ab45178; Abcam, Cambridge, UK). The appropriate secondary ABs, goat anti-rabbit IgG H&L (HRP) (1:5000, ab205718; Abcam, Cambridge, UK) and goat anti-mouse IgG H&L (HRP) (1:5000, ab205719; Abcam, Cambridge, UK), were added following three rounds of washing with TBS-T. The ABs were then incubated for 1 h at ambient temperature. Subsequent to the washing with TBS-T, the immunoreactive bands were identified and captured using a Chemiluminescence Imaging System (Chemiscope 3000; Shanghai Qinxiang Scientific Instrument Co, Ltd., Shanghai, China).

Immunofluorescence

Proteins in the cell lines were localized with immunofluorescence. Subsequently, the slides were eliminated and fixed with 4% paraformaldehyde for a duration of 10 min. In summary, the cells were cultivated on glass coverslips and then

fixed in a solution containing 4% paraformaldehyde for 30 min at ambient temperature. Afterward, they were subjected to a 0.5% Triton X-100 solution for an interval of 20 min. The cells were afterward treated with a solution containing 1% bovine serum albumin at ambient temperature for 1 h in order to hinder any non-specific binding. Lastly, the cells were incubated overnight at 4°C with a solution incorporating 2 μg/mL of both anti-ASK1/PGAM5 ABs. The cells were rinsed with PBS and then incubated at 2 μg/mL of goat anti-rabbit (ab150077) and -mouse (ab150116) IgG H&L (Alexa Fluor® 488 and 594) (Abcam, Cambridge, UK) at 37 °C for a duration of 1 h, while being kept in darkness. The nuclei were labeled with 4′,6-diamidino-2-phenylindole (DAPI). The slides were coated with a solution containing 50% glycerol. The ASK1 and PGAM5 proteins were examined for their expression and localization with a laser confocal microscopy (Eclipse TS100-F; Nikon Corporation, Japan). The fluorescence intensity was estimated utilizing the ImageJ program.

Data Analysis

Values reported for all data are shown as mean ± standard deviation. SPSS19.0 software was deployed for statistical analysis of the data of each group, and one-way analysis of variance was used for statistics. Significance was deemed at $P < 0.05$. GraphPad Prism 9.5.1 was implemented for mapping.

Results

Patients with COPD Had Increased PGAM5 Expression and Numbers of M1 Cells

Significant pathological differences were observed between the control and COPD groups. H&E staining of lung tissues from patients with COPD revealed fusion of alveoli with a higher mean linear intercept than that of the controls (Figure 1A and B). Furthermore, we estimated the PGAM5, CD86, and CD206 expressions with IHC staining. Contrasted with the control group, COPD patients lung tissues experienced an elevation in PGAM5 expression, and the expression for the CD86 marker for M1 macrophages was increased, whereas the CD206 expression, an indicator for M2 macrophages, was reduced (Figure 1C–H). To investigate the role of PGAM5 and macrophage polarization in the pathogenesis of COPD, double immunofluorescence staining was used to co-label PGAM5 expression and M1/M2 macrophage markers in human lung tissue. The results showed that the rate of double-label positivity for $CD86^{+}PGAM5^{+}$ was higher in the COPD group than in the smoker control group, but the double-label positivity for $CD206^{+}PGAM5^{+}$ did not show a significant difference between the COPD group and the smoker control group (Figure 1I–L).

CSE Led to Increased PGAM5 Expression in Macrophages, an Elevation in M1, and Hindrance in M2 Macrophages

We exposed the MH-S cells to either saline or CSE for a duration of 24 h. Moreover, we ascertained PGAM5 expression with Western blot analysis, whereas we determined the quantity of M1/2 macrophages using flow cytometry. The CSE group possessed an elevated PGAM5 expression (Figure 2A and B). This boost was followed by a rise in the population of M1 macrophages (Figure 2C and D) and a reduction in the number of M2 macrophages (Figure 2E and F).

PGAM5 Knockdown Reversed CSE-Induced M1 Macrophage Polarization and Reduced Inflammatory Factor Expression

We allocated MH-S cells into four groups in order to further ascertain the PGAM5 implication on macrophage polarization. The first group served as the control, consisting of cells gathered after 24 h of normal incubation. The second group referred to as the CSE group, involved cells treated with 5% CSE for 24 h. The third group, known as the CSE+siRNA-NC group, included cells transfected with siRNA-negative control for 24 h, followed by treatment with 5% CSE for 24 h. Lastly, the fourth group, referred to as the CSE+PGAM5-siRNA group, consisted of cells transfected with siRNA-PGAM5-257, followed by treatment with 5% CSE for 24 h. We ascertained the positivity rates of M1/2 macrophages with the flow cytometry. Additionally, we estimated the inflammatory cytokines IL-1β, TNF-α, TGF-β1, and IL-10 expression levels with the ELISA method. The outcomes demonstrated that CSE administration led to an upregulation of M1 macrophage expression and a downregulation of M2 macrophage expression (Figure 3A–C). CSE also caused changes in the inflammatory factors expression levels, with elevated

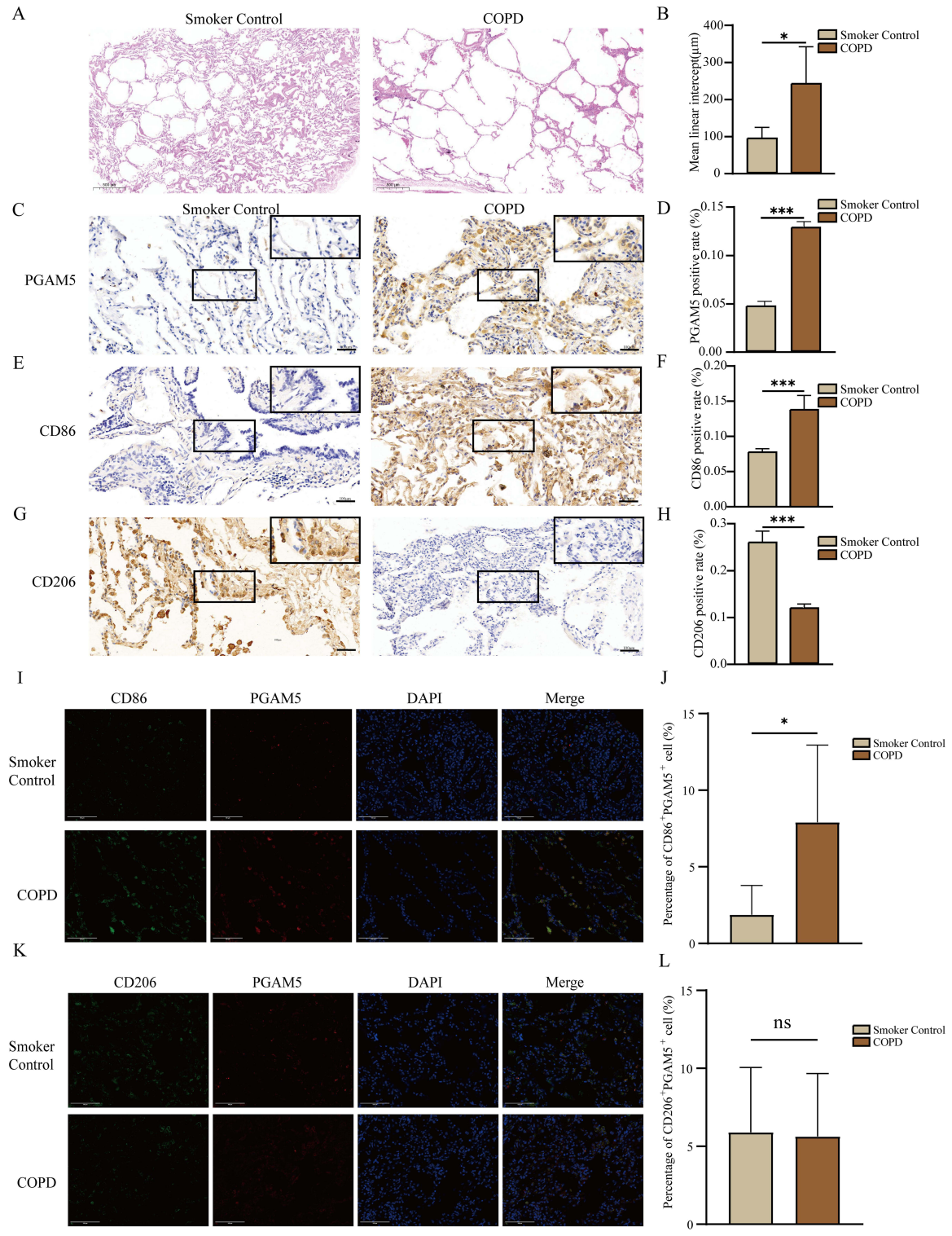

Figure 1 Differences in lung tissue structure and PGAM5 and CD86/206 expression levels in COPD patients and Smoker controls. (**A** and **B**) H&E staining of lung tissue in COPD patients and the smoker control group, and between-group differences in MLI. Magnification 4×, scale bar: 500 μM. (**C–H**) Expression of PGAM5, CD86, and CD206 in the lung tissues of patients with COPD and without COPD. Representative IHC staining (200×, scale bars: 100 μm) and measurement of positivity rate. (**I-L**) Immunofluorescence staining for the distribution of PGAM5, CD86 and CD206 in lung tissues. Representative photomicrographs of double-labeled immunofluorescence staining of PGAM5 (red), CD86/CD206 (green) and nucleus (blue) in human lung tissue, images were observed by laser confocal microscopy. (magnification, 40×,scale bars: 100 μm). The percentage of double-label positive cells was calculated in Image J software. Values are mean ± SD of three replications; Smoker controls n = 4, COPD group n = 9. (*P < 0.05, ***P < 0.001).

Abbreviations: COPD, chronic obstructive pulmonary disease; H&E, Hematoxylin and eosin; MLI, mean linear intercept; IHC, immunohistochemical; SD, standard deviation.

https://doi.org/10.2147/COPD.S492627

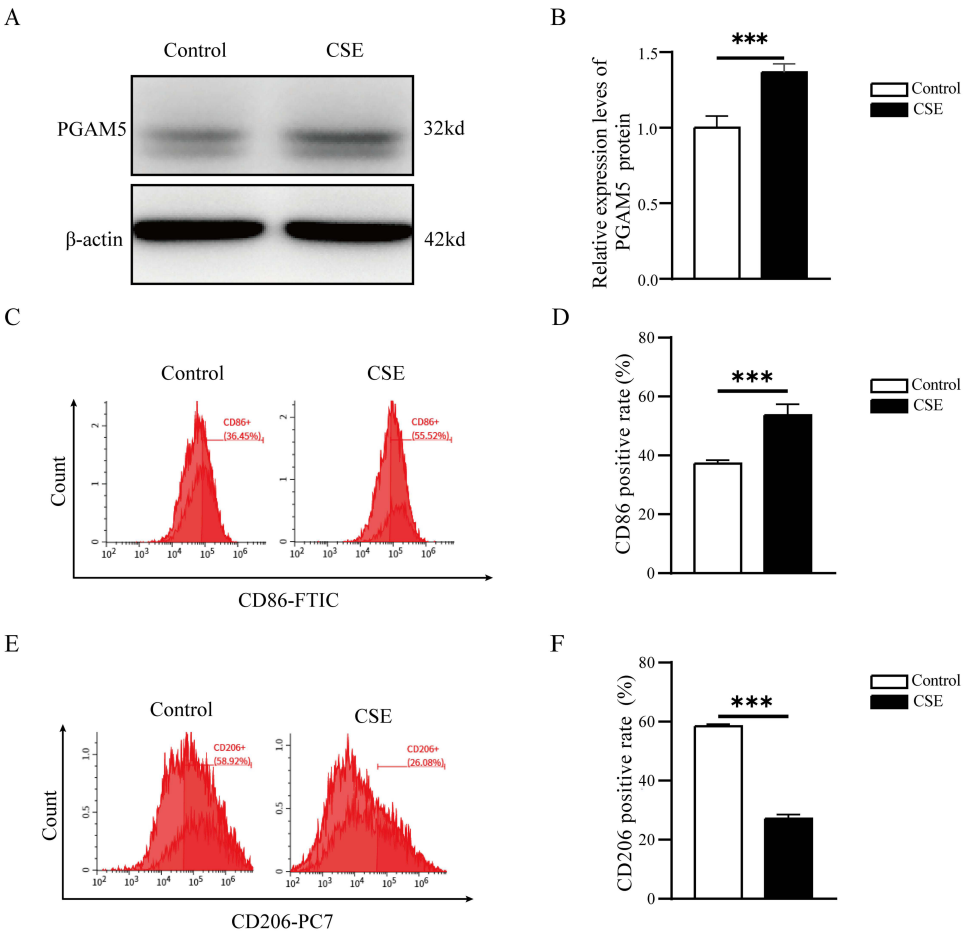

Figure 2 CSE increased the PGAM5 expression and M1 macrophages and mitigated the expression of M2 macrophages. (**A** and **B**) PGAM5 protein expression. (**C-F**) Differences in CD86 and CD206 expression between the CSE treatment and control groups. Values are mean ± SD of three replications. (***P < 0.001).
Abbreviations: CSE, Cigarette smoke extract; SD, standard deviation.

IL-1 β, TNF- α, and TGF- β1 levels and mitigated IL-10 levels (Figure 3D–G). These results were reversed after the PGAM5 knockdown.

PGAM5 Activated ASK1 and NF-κB Pathways

Furthermore, we quantified the p-ASK1 and NF-κB pathway protein expression in MH-S cells with Western blotting to ascertain the mechanism of PGAM5-induced macrophage polarization. The outcomes reported that CSE increased the PGAM5 and p-ASK1^{T838} expression levels in MH-S cells; however, the p-ASK1^{ser1029} levels decreased and there was no significant difference in the expression level of ASK1 among all groups (Figure 4A–E). In addition, CSE increased p-p65 expression, but P65 expression was constant (Figure 4F and G). When PGAM5 was silenced, the level of p-ASK1^{ser1029} returned to its initial level, and the expression of p-ASK1^{T838} and p-p65 decreased. To substantiate this conclusion, we performed rescue experiments. See Supplementary Figure 2 for rescue experiments.

PGAM5 Co-Localizes and Combines with ASK1

Subsequently, we investigated the interactions between PGAM5 and ASK1 and detected the expression and co-localization of PGAM5 and ASK1 using immunofluorescence. This result indicated that CSE treatment raised the PGAM5 and ASK1 expression level and co-localization; when PGAM5 was knocked down, the fluorescence intensity of ASK1 and PGAM5 decreased, and co-localization was reduced (Figure 5A and B). Co-IP experiments also confirmed that PGAM5 and ASK1 could bind to each other (Figure 5C).

https://doi.org/10.2147/COPD.S492627

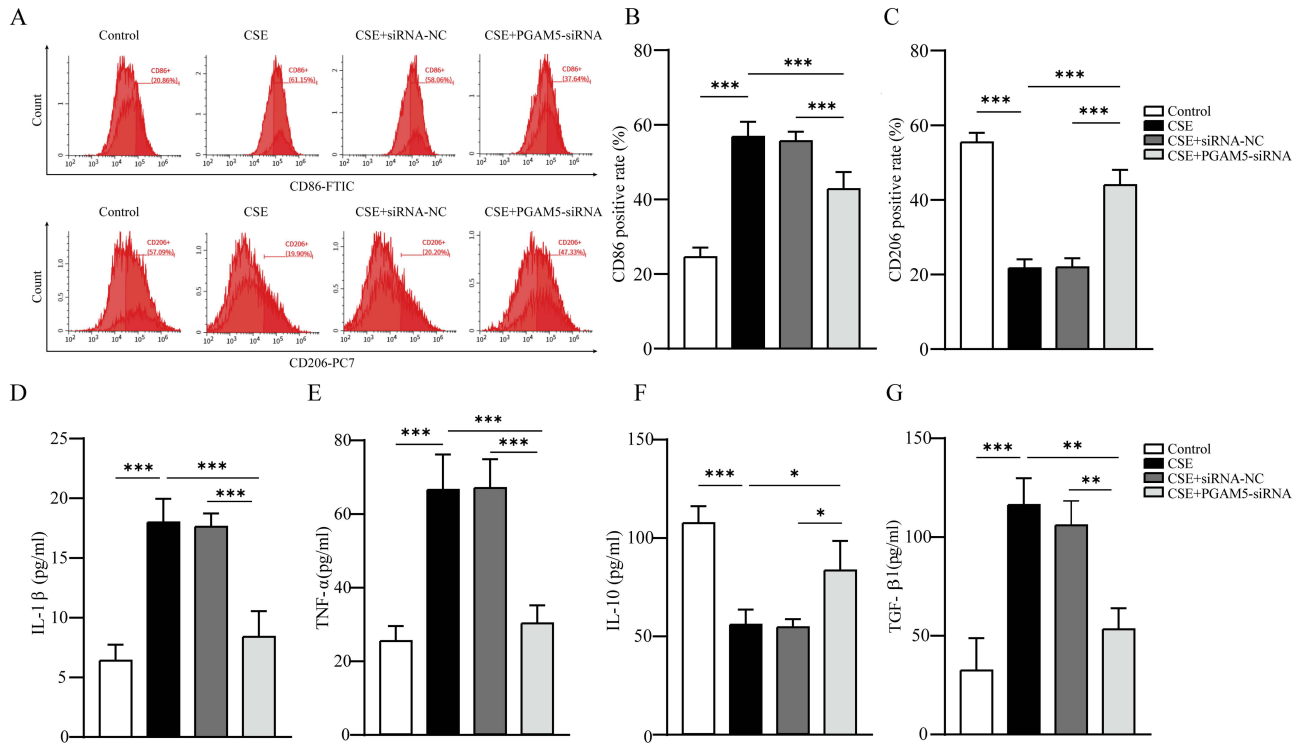

Figure 3 Number of M1/2 macrophages and expression of inflammatory factors among the various groups. (**A**) CD86/206 expression levels in various treatment groups. (**B** and **C**) CD86 and CD206 positivity rates in different treatment groups. (**D**–**G**) IL-1β, TNF-α, IL-10, and TGF-β1 expression levels. Values are mean ± SD of three replications (*P < 0.05, **P < 0.01, ***P < 0.001).

Abbreviations: CSE, cigarette smoke extract; SD, standard deviation.

Discussion

Smoking is widely known to be the primary cause of COPD, with inflammation being a key factor in its development.[27] Smoke's toxic components may trigger the antigen-presenting cells activation, resulting in the T-helper-1 (Th1) cells activation. This activation can impact macrophage polarization and the release of inflammatory factors.[18,28,29] Macrophages are the primary immune cells found in the lungs and possess a crucial function in initiating inflammation. They may be polarized to M1 /2 macrophages.[30] M1-type macrophages induce inflammation, whereas M2-type macrophages mitigate it.[31,32] PGAM5 is an exceptional Ser/Thr-specific phosphatase and has been shown to be closely related to inflammation.[33] Moreover, Ng Kee Kwong et al reported that the lungs of COPD patients possessed an elevated PGAM5 expression.[19] Our results were consistent with the results of their investigation. We reported that PGAM5 had an elevated expression in the COPD patients' lung tissues, which was accompanied by alveolar rupture and fusion. Importantly, we also found that PGAM5 was expressed in lung macrophages, and COPD group had significant upregulation of PGAM5 expression, which was concomitant with an elevation in CD86 expression, a recognized indicator of M1 macrophages.[34] Thus, we posit that there is a strong correlation between PGAM5 and both macrophage polarization and the development of COPD.

Liu et al indicated that PGAM5 is closely related to macrophage polarization in osteoarthritis.[35] Herein, we observed an elevation of PGAM5 expression in CSE-treated MH-S cells, followed with a rise in M1 macrophages and a reduction in M2 macrophages. We silenced *PGAM5* to further verify the role of PGAM5 and found that when *PGAM5* was silenced, the M1 macrophage's polarization decreased, and that of M2 macrophages increased. Concurrently, we found that the rise in PGAM5 coincided with an elevation in the inflammatory cytokines IL-1β and TNF-α release by M1 macrophages, whereas there was a decline in the secretion of IL-10 by M2 macrophages. These results align with those of studies conducted by Sun and Feng.[12,36] This confirmed our hypothesis that PGAM5 is closely related to macrophage polarization and secretion of inflammatory factors in COPD and that silencing PGAM5 can reverse the effect of CSE on macrophages. Our study also revealed unexpected changes in the TGF-β1 levels. TGF-β1 belongs to the TGF-β protein

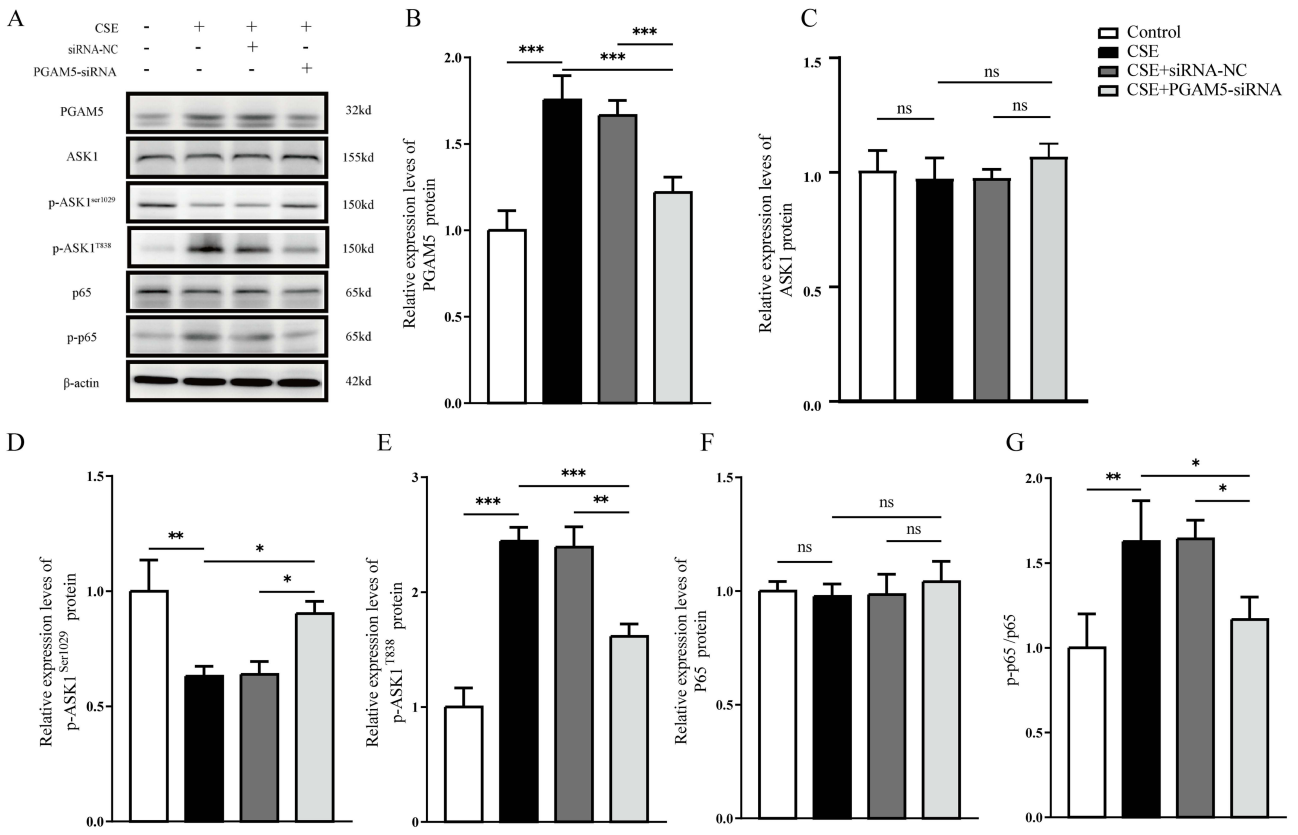

Figure 4 PGAM5 associates with ASK1 and NF-κB pathways. (**A**) Expression of PGAM5, ASK1, p-ASK1ser1029, p-ASK1T838, p65, and p-p65 in MH-S cells. (**B**–**G**) Quantification of WB results in (**A**). Data were expressed as the means ± SD of triplicate experiments. (*P < 0.05, **P < 0.01, ***P < 0.001).
Abbreviations: CSE, cigarette smoke extract; MH-S, mouse alveolar macrophage; WB, Western blotting; SD, standard deviation.

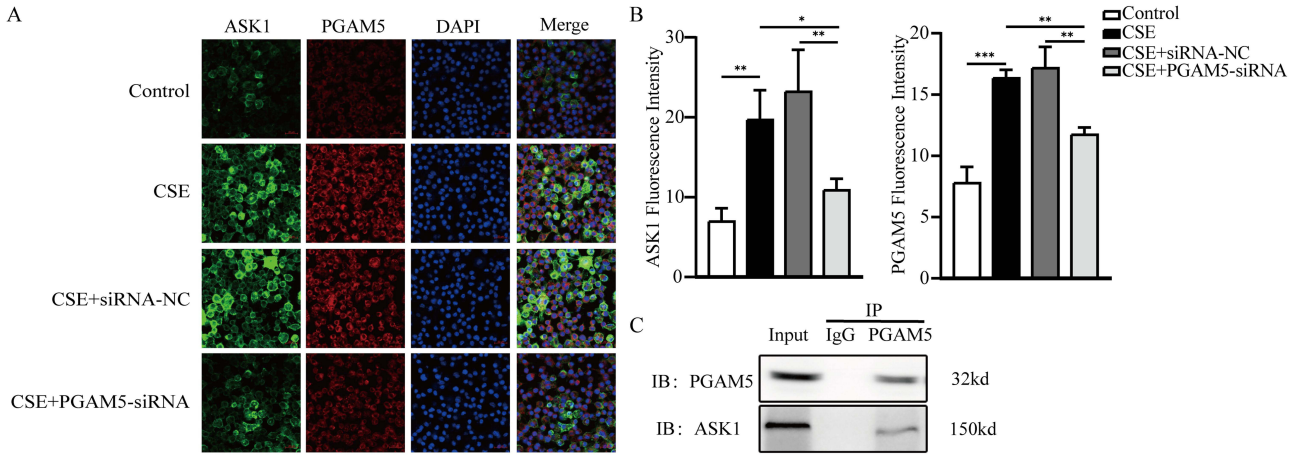

Figure 5 PGAM5 co-localizes and combines with ASK1. (**A**) ASK1 and PGAM5 protein expression and localization were observed using laser confocal microscopy (original magnification ×200; scale bars=20 μm). Green: ASK1 immunofluorescence; red: PGAM5 immunofluorescence; blue: DAPI. (**B**) Fluorescence intensity expression levels of ASK1 and PGAM5 proteins in various treatment groups of cells. (**C**) Co-immunoprecipitation assays. Data were expressed as the means ± SD of triplicate experiments. (*P < 0.05. **P < 0.01,***P < 0.001).
Abbreviation: SD, standard deviation.

family, which possesses an significant function in controlling cell proliferation and differentiation, wound healing, and the immune system.[37] In the MH-S cells treated with CSE, the TGF-β1 expression level associated with M2-type macrophages increased. This could be associated with airway remodeling in COPD patients. Mihara et al showed that the bronchial epithelial cells function as the primary anatomical barrier against noxious gasses and cigarette smoke particles.

https://doi.org/10.2147/COPD.S492627

CSE triggers the reactive oxygen species generation inside the cells and the subsequent release of TGF-β1, inducing epithelial-mesenchymal transition in differentiated bronchial epithelial cells, leading to airway remodeling in COPD.[38,39] Therefore, a similar mechanism may exist in MH-S cells, resulting in an increase in TGF-β1 levels in the CSE-treated group. However, the specific mechanisms involved require further investigation. Collectively, these outcomes suggest that PGAM5 stimulates M1 macrophage polarization and secretion of proinflammatory factors.

Previous studies have shown that PGAM5 expression correlates with ASK1 expression. Sadatomi et al demonstrated that elevated PGAM5 levels stimulate the ASK1-JNK and ASK1-38 pathways, and the reduction of PGAM5 levels mitigated the ASK1 fundamental activity.[40] Ding and Takeda revealed that PGAM5 influences the phosphorylation of ASK1.[41,42] ASK1 is a protein kinase that triggers cell division and serves as a crucial sensor of cellular stress.[43] ASK1 is commonly triggered in living organisms with oxidative stress and contributes to oxidative damage,[44,45] and is strongly associated with the signaling pathways activation that participate in cell death, inflammation, and fibrosis.[46] Prior investigations also have demonstrated that distinct mechanisms govern the ASK1 phosphorylation in response to various stimulators, and within the ASK1 kinase domain, different loci have diverse functions, including inhibition and activation. Thr-838 phosphorylation activates ASK1,[42,47] whereas the serine residues phosphorylation at Ser-83/966 possesses a contrasting impact.[43] Agrahari et al demonstrated that PGAM5 dephosphorylates ASK1 inhibitory phosphorylation sites other than Ser-83/966/1033, leading to ASK1 activation.[47,48] Ser-1036/Ser-1040 (Ser-1029/Ser-1033 in humans) is linked to the suppression of ASK1 pro-apoptotic activity.[49] The exact location of PGAM5 phosphorylation of ASK1 remains unknown, and our results also suggest that the effect of PGAM5 on ASK1 varies for different sites. Our experimental findings showed that high PGAM5 expression led to increased p-ASK1^{T838} expression and decreased p-ASK1^{ser1029} expression. These results indicated that PGAM5 may activate ASK1 in this manner.

Additionally, ASK1 activation contributes to the NF-κB pathway activation, which is essential for regulating the immune system and macrophage polarization.[50–52] The inflammatory cytokines and *NF-κB* mRNA levels are major factors in COPD.[53] Within the cytoplasm, NF-κB is present as either heterodimers or homodimers,[16,54] NF-κB is commonly present in cells in a dimeric state, with the p65/p50 heterodimer being the most common. p50 contains nuclear localization signals and is the binding site between nuclear factors and DNA. As the most important functional subunit, p65 has a special transactivation domain (TAD), may control the process of transcribing numerous downstream target genes and participates in various important cellular life activities.[55–58] The serine at position 536 (Ser-536) located in the TAD domain is highly conserved in p65. Phosphorylation is catalyzed by various kinases that exert different biological effects. Currently, the phosphorylation modification of Ser-536 is the most studied modification site in p65, and p65 phosphorylation can enhance NF-κB transcriptional activation. Phosphorylation of p65 can be achieved without relying on IκB and participates in the regulation of NF-κB.[55,59–61] Our findings indicate that CSE treatment leads to an increase in p-p65 and activates the NF-κB signaling pathway, and these effects are reversed after PGAM5 silencing. Co-IP and immunofluorescence experiments verified that PGAM5 and ASK1 bind to each other. These outcomes were aligned with those of prior investigations. Hence, we suggest that the combination of PGAM5 and ASK1 is responsible for the NF-κB pathway activation and COPD development.

These findings advance the research on the molecular basis of COPD, which is crucial for developing new treatment goals and drugs and refining clinical therapeutic strategies. However, PGAM5 acts as a phosphorylase, and the reason it can increase the phosphorylation levels of ASK1^{T838} is unknown; in addition, this present study was obtained mainly from MH-S cells, and there is a lack of in vivo experimental data, and due to the difficulty in obtaining human lung tissue, the number of human lung tissue specimens in this study is relatively small. Therefore, Further studies are needed to investigate this further.

Conclusion

PGAM5 can cause an increase in p-ASK1^{T838}, contributing to the ASK1 activation and activating the NF-κB pathway, causing macrophages to polarize into M1 macrophages and stimulating the generation of proinflammatory factors TNF-α and IL-1β (Figure 6). This process contributes to COPD development. The outcomes of our investigation demonstrate the role of PGAM5 in COPD development and advancement. We offer valuable insights and novel concepts for the

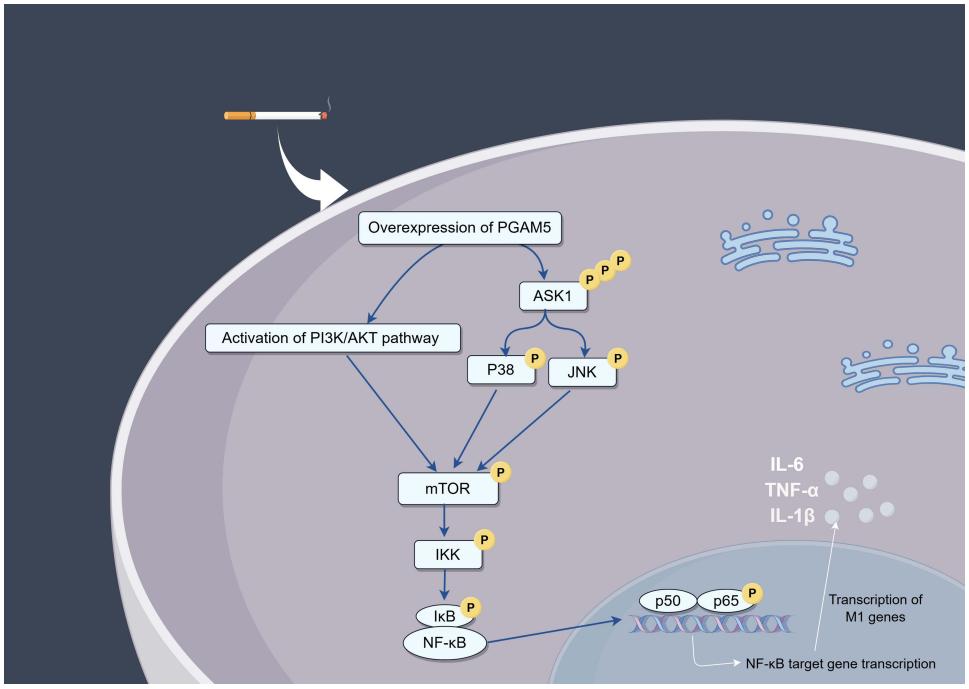

Figure 6 Schematic representation of PGAM5 activating NF-κB signaling pathway to promote polarization of M1 macrophages. PGAM5 can enhance the phosphorylation of ASK1, and phosphorylated ASK1 can activate the downstream p38 and JNK pathways, leading to the activation of mTOR. Activated mTOR can promote the phosphorylation of IKK, which in turn phosphorylates IκB and dissociates it from NF-κB, resulting in the activation and translocation of NF-κB into the nucleus, initiating related gene transcription, leading to the polarization of M1 macrophages and the secretion of pro-inflammatory factors such as IL-1β and TNF-α.
Abbreviations: PGAM5, phosphoglycerate mutase 5; PI3K, phosphoinositide 3-kinase; AKT, protein kinase B; p38, p38 MAPK; JNK, c-Jun N-terminal kinase; mTOR, mechanistic target of rapamycin; IKK, inhibitor of kappa B kinase; NF-κB, nuclear factor kappa-B; Inhibitor of nuclear factor kappa-B; IL-6, interleukin 6; TNF-α, Tumour necrosis factor-alpha; IL-1β, Interleukin-1beta.

identification of creative strategies for preventing and treating COPD. These findings have important implications for future efforts in preventing and treating COPD.

Data Sharing Statement

All data produced or examined throughout this investigation are encompassed in this published paper and its Supplementary Information Files.

Ethics Approval and Consent to Participate

This investigation was conducted aligning with the Declaration of Helsinki and approved by the Ethics Committee of the Second Affiliated Hospital of Hainan Medical University (No. LW2022178). All the subjects offered informed consent. The nine lung transplant patients were all voluntarily donated with informed consent, and that these were conducted in accordance with the Declaration of Istanbul.

Acknowledgments

We would like to express our gratitude to all the volunteers who contributed to the successful completion of this research.

Author Contributions

All authors made a significant contribution to the work reported, whether that is in the conception, study design, execution, acquisition of data, analysis and interpretation, or in all these areas; took part in drafting, revising or critically reviewing the article; gave final approval of the version to be published; have agreed on the journal to which the article has been submitted; and agree to be accountable for all aspects of the work.

Funding

This project was financially supported by the Hainan Province Clinical Medical Center, the National Natural Science Foundation of China (No. 81760005), the Natural Science Foundation of Hainan Province (Nos. 822QN471 and 821QN408), and the Open Foundation of the NHC Key Laboratory of Tropical Disease Control, Hainan Medical University (2020-PT310-009).

Disclosure

The authors report no conflicts of interest in this work.

References

1. Lahmar Z, Ahmed E, Fort A, Vachier I, Bourdin A, Bergougnoux A. Hedgehog pathway and its inhibitors in chronic obstructive pulmonary disease (COPD). *Pharmacol Ther*. 2022;240:108295. doi:10.1016/j.pharmthera.2022.108295
2. Kwak N, Lee KH, Woo J, et al. Del-1 Plays a Protective Role against COPD Development by Inhibiting Inflammation and Apoptosis. *Int J mol Sci*. 2024;25(4):1955. doi:10.3390/ijms25041955
3. Singh D, Criner GJ, Agusti A, et al. Benralizumab prevents recurrent exacerbations in patients with chronic obstructive pulmonary disease: a post hoc analysis. *Int J Chron Obstruct Pulmon Dis*. 2023;18:1595–1599. doi:10.2147/COPD.S418944
4. Liu J, Zhang Z, Yang Y, Di T, Wu Y, Bian T. NCOA4-mediated ferroptosis in bronchial epithelial cells promotes macrophage M2 polarization in COPD emphysema. *Int J Chron Obstruct Pulmon Dis*. 2022;17:667–681. doi:10.2147/COPD.S354896
5. Liu Y, Liu H, Li C, Ma C, Ge W. Proteome profiling of lung tissues in chronic obstructive pulmonary disease (COPD): platelet and macrophage dysfunction contribute to the pathogenesis of COPD. *Int J Chron Obstruct Pulmon Dis*. 2020;15:973–980. doi:10.2147/copd.S246845
6. Le Y, Cao W, Zhou L, et al. Infection of mycobacterium tuberculosis promotes both M1/M2 polarization and MMP production in cigarette smoke-exposed macrophages. *Front Immunol*. 2020;11:1902. doi:10.3389/fimmu.2020.01902
7. Kim GD, Lim EY, Shin HS. Macrophage polarization and functions in pathogenesis of chronic obstructive pulmonary disease. *Int J mol Sci*. 2024;25(11). doi:10.3390/ijms25115631
8. Chen X, Deng Q, Li X, Xian L, Xian D, Zhong J. Natural plant extract - loganin: a hypothesis for psoriasis treatment through inhibiting oxidative stress and equilibrating immunity via regulation of macrophage polarization. *Clin Cosmet Invest Dermatol*. 2023;16:407–417. doi:10.2147/CCID.S396173
9. Chen Y, Yang L, Li X. Advances in mesenchymal stem cells regulating macrophage polarization and treatment of sepsis-induced liver injury. *Front Immunol*. 2023;14:1238972. doi:10.3389/fimmu.2023.1238972
10. Liu T, Zhang Z, Shen W, Wu Y, Bian T. MicroRNA Let-7 induces M2 macrophage polarization in COPD emphysema through the IL-6/STAT3 pathway. *Int J Chron Obstruct Pulmon Dis*. 2023;18:575–591. doi:10.2147/COPD.S404850
11. Xiong K, Ao K, Wei W, et al. Periodontitis aggravates COPD through the activation of γδ T cell and M2 macrophage. *mSystems*. 2024;9(2):e0057223. doi:10.1128/msystems.00572-23
12. Sun X, Liu Y, Feng X, Li C, Li S, Zhao Z. The key role of macrophage depolarization in the treatment of COPD with ergosterol both in vitro and in vivo. *Int Immunopharmacol*. 2020;79:106086. doi:10.1016/j.intimp.2019.106086
13. Feng H, Zhang D, Yin Y, Kang J, Zheng R. Salidroside ameliorated the pulmonary inflammation induced by cigarette smoke via mitigating M1 macrophage polarization by JNK/c-Jun. *Phytother Res*. 2023;37(9):4251–4264. doi:10.1002/ptr.7905
14. Z K, D R, Y Y, et al. Cigarette smoke-induced lung inflammation in COPD mediated via CCR1/JAK/STAT /NF-κB pathway. *Aging*. 2020;12(10):9125–9138. doi:10.18632/aging.103180
15. Luo F, Li H, Ma W, et al. The BCL-2 inhibitor APG-2575 resets tumor-associated macrophages toward the M1 phenotype, promoting a favorable response to anti-PD-1 therapy via NLRP3 activation. *Cell mol Immunol*. 2024;21(1):60–79. doi:10.1038/s41423-023-01112-y
16. Chen M, Zhang Y, Zhou P, et al. Substrate stiffness modulates bone marrow-derived macrophage polarization through NF-kappaB signaling pathway. *Bioact Mater*. 2020;5(4):880–890. doi:10.1016/j.bioactmat.2020.05.004
17. Wang Y, Wang X-K, Wu -P-P, Wang Y, Ren L-Y, Xu A-H. Necroptosis mediates cigarette smoke-induced inflammatory responses in macrophages. *Int J Chron Obstruct Pulmon Dis*. 2020;15:1093–1101. doi:10.2147/copd.S233506
18. Li Z, Li L, Lv X, Hu Y, Cui K. Ginseng saponin Rb1 attenuates cigarette smoke exposure-induced inflammation, apoptosis and oxidative stress via activating Nrf2 and inhibiting NF-κB signaling pathways. *Int J Chron Obstruct Pulmon Dis*. 2023;18:1883–1897. doi:10.2147/copd.S418421
19. Ng Kee Kwong F, Nicholson AG, Pavlidis S, Adcock IM, Chung KF. PGAM5 expression and macrophage signatures in non-small cell lung cancer associated with chronic obstructive pulmonary disease (COPD). *BMC Cancer*. 2018;18(1):1238. doi:10.1186/s12885-018-5140-9
20. Ruiz K, Thaker TM, Agnew C, et al. Functional role of PGAM5 multimeric assemblies and their polymerization into filaments. *Nat Commun*. 2019;10(1):531. doi:10.1038/s41467-019-08393-w
21. Bang B-R, Miki H, Kang YJ. Mitochondrial PGAM5−Drp1 signaling regulates the metabolic reprogramming of macrophages and regulates the induction of inflammatory responses. *Front Immunol*. 2023;14:1243548. doi:10.3389/fimmu.2023.1243548
22. Kang TB, Yang SH, Toth B, Kovalenko A, Wallach D. Caspase-8 blocks kinase RIPK3-mediated activation of the NLRP3 inflammasome. *Immunity*. 2013;38(1):27–40. doi:10.1016/j.immuni.2012.09.015
23. Moriwaki K, Farias Luz N, Balaji S, et al. The mitochondrial phosphatase PGAM5 is dispensable for necroptosis but promotes inflammasome activation in macrophages. *J Immunol*. 2016;196(1):407–415. doi:10.4049/jimmunol.1501662
24. Dai WL, Bao YN, Fan JF, et al. Levo-corydalmine attenuates microglia activation and neuropathic pain by suppressing ASK1-p38 MAPK/NF-kappaB signaling pathways in rat spinal cord. *Reg Anesth Pain Med*. 2020;45(3):219–229. doi:10.1136/rapm-2019-100875
25. Su X, Chen J, Lin X, et al. FERMT3 mediates cigarette smoke-induced epithelial–mesenchymal transition through Wnt/β-catenin signaling. *Respir Res*. 2021;22(1). doi:10.1186/s12931-021-01881-y

26. Hong J. Protective effects of curcumin-regulated intestinal epithelial autophagy on inflammatory bowel disease in mice. *Gastroenterol Res Pract*. 2022;2022:2163931. doi:10.1155/2022/2163931
27. Chen P, Li Y, Wu D, Liu F, Cao C. Secondhand smoke exposure and the risk of chronic obstructive pulmonary disease: a systematic review and meta-analysis. *Int J Chron Obstruct Pulmon Dis*. 2023;18:1067–1076. doi:10.2147/COPD.S403158
28. Chen G, Mu Q, Meng Z-J. Cigarette smoking contributes to Th1/Th2 cell dysfunction via the cytokine milieu in chronic obstructive pulmonary disease. *Int J Chron Obstruct Pulmon Dis*. 2023;18:2027–2038. doi:10.2147/copd.S426215
29. Cutolo M, Campitiello R, Gotelli E, Soldano S. The role of M1/M2 macrophage polarization in rheumatoid arthritis synovitis. *Front Immunol*. 2022;13:867260. doi:10.3389/fimmu.2022.867260
30. Wynn TA, Vannella KM. Macrophages in tissue repair, regeneration, and fibrosis. *Immunity*. 2016;44(3):450–462. doi:10.1016/j.immuni.2016.02.015
31. Dewhurst JA, Lea S, Hardaker E, Dungwa JV, Ravi AK, Singh D. Characterisation of lung macrophage subpopulations in COPD patients and controls. *Sci Rep*. 2017;7(1):7143. doi:10.1038/s41598-017-07101-2
32. Hu T, Pang N, Li Z, et al. The activation of M1 macrophages is associated with the JNK-m6A-p38 axis in chronic obstructive pulmonary disease. *Int J Chron Obstruct Pulmon Dis*. 2023;18:2195–2206. doi:10.2147/copd.S420471
33. Luz NF, Khouri R, Van Weyenbergh J, et al. Leishmania braziliensis subverts necroptosis by modulating RIPK3 expression. *Front Microbiol*. 2018;9:2283. doi:10.3389/fmicb.2018.02283
34. Xu G, Mo Y, Li J, Wei Q, Zhou F, Chen J. Two tripartite classification systems of CD86(+) and CD206(+) macrophages are significantly associated with tumor recurrence in stage II-III colorectal cancer. *Front Immunol*. 2023;14:1136875. doi:10.3389/fimmu.2023.1136875
35. Liu Y, Hao R, Lv J, et al. Targeted knockdown of PGAM5 in synovial macrophages efficiently alleviates osteoarthritis. *Bone Res*. 2024;12(1):15. doi:10.1038/s41413-024-00318-8
36. Feng H, Yin Y, Ren Y, et al. Effect of CSE on M1/M2 polarization in alveolar and peritoneal macrophages at different concentrations and exposure in vitro. *Vitro Cell Dev Biol Anim*. 2020;56(2):154–164. doi:10.1007/s11626-019-00426-4
37. Cai G, Lu Y, Zhong W, et al. Piezo1-mediated M2 macrophage mechanotransduction enhances bone formation through secretion and activation of transforming growth factor-beta1. *Cell Prolif*. 2023;56(9):e13440. doi:10.1111/cpr.13440
38. Milara J, Peiro T, Serrano A, Cortijo J. Epithelial to mesenchymal transition is increased in patients with COPD and induced by cigarette smoke. *Thorax*. 2013;68(5):410–420. doi:10.1136/thoraxjnl-2012-201761
39. Guan R, Wang J, Cai Z, et al. Hydrogen sulfide attenuates cigarette smoke-induced airway remodeling by upregulating SIRT1 signaling pathway. *Redox Biol*. 2020;28:101356. doi:10.1016/j.redox.2019.101356
40. Sadatomi D, Tanimura S, Ozaki K, Takeda K. Atypical protein phosphatases: emerging players in cellular signaling. *Int J mol Sci*. 2013;14(3):4596–4612. doi:10.3390/ijms14034596
41. Ding MJ, Fang HR, Zhang JK, et al. E3 ubiquitin ligase ring finger protein 5 protects against hepatic ischemia reperfusion injury by mediating phosphoglycerate mutase family member 5 ubiquitination. *Hepatology*. 2022;76(1):94–111. doi:10.1002/hep.32226
42. Takeda. K, Komuro. Y, Hayakawa. T, et al. Mitochondrial phosphoglycerate mutase 5 uses alternate catalytic activity as a protein serine/threonine phosphatase to activate ASK1. *Proc Natl Acad Sci U S A*. 2009;106(30):12301–12305. doi:10.1073/pnas.0901823106
43. Morales Betanzos C, Federspiel JD, Palubinsky AM, McLaughlin B, Liebler DC. Dynamic phosphorylation of apoptosis signal regulating kinase 1 (ASK1) in response to oxidative and electrophilic stress. *Chem Res Toxicol*. 2016;29(12):2175–2183. doi:10.1021/acs.chemrestox.6b00339
44. Zhou J, Shao Z, Kerkela R, et al. Serine 58 of 14-3-3zeta is a molecular switch regulating ASK1 and oxidant stress-induced cell death. *mol Cell Biol*. 2009;29(15):4167–4176. doi:10.1128/MCB.01067-08
45. Obsilova V, Honzejkova K, Obsil T. Structural insights support targeting ASK1 kinase for therapeutic interventions. *Int J mol Sci*. 2021;22(24):13395. doi:10.3390/ijms222413395
46. Liles JT, Corkey BK, Notte GT, et al. ASK1 contributes to fibrosis and dysfunction in models of kidney disease. *J Clin Invest*. 2018;128(10):4485–4500. doi:10.1172/JCI99768
47. Nishida T, Hattori K, Watanabe K. The regulatory and signaling mechanisms of the ASK family. *Adv Biol Regul*. 2017;66:2–22. doi:10.1016/j.jbior.2017.05.004
48. Agrahari AK, Dikshit M, Asthana S. Crystallographic mining of ASK1 regulators to unravel the intricate PPI interfaces for the discovery of small molecule. *Comput Struct Biotechnol J*. 2022;20:3734–3754. doi:10.1016/j.csbj.2022.07.008
49. Singh V, Huang E, Pathak V, Willard BB, Allende DS, Nagy LE. Phosphoproteomics identifies pathways underlying the role of receptor-interaction protein kinase 3 in alcohol-associated liver disease and uncovers apoptosis signal-regulating kinase 1 as a target. *Hepatol Commun*. 2022;6(8):2022–2041. doi:10.1002/hep4.1956
50. Jiao B, An C, Tran M, et al. Pharmacological inhibition of STAT6 ameliorates myeloid fibroblast activation and alternative macrophage polarization in renal fibrosis. *Front Immunol*. 2021;12:735014. doi:10.3389/fimmu.2021.735014
51. Yang SR, Yao H, Rajendrasozhan S, et al. RelB is differentially regulated by IkappaB Kinase-alpha in B cells and mouse lung by cigarette smoke. *Am J Respir Cell mol Biol*. 2009;40(2):147–158. doi:10.1165/rcmb.2008-0207OC
52. Wang Y, Zhou J-S, Xu X-C, et al. Endoplasmic reticulum chaperone GRP78 mediates cigarette smoke-induced necroptosis and injury in bronchial epithelium. *Int J Chron Obstruct Pulmon Dis*. 2018;13:571–581. doi:10.2147/copd.S150633
53. Zhou L, Liu Y, Chen X, et al. Over-expression of nuclear factor-κB family genes and inflammatory molecules is related to chronic obstructive pulmonary disease. *Int J Chron Obstruct Pulmon Dis*. 2018;13:2131–2138. doi:10.2147/copd.S164151
54. Alharbi KS, Fuloria NK, Fuloria S, et al. Nuclear factor-kappa B and its role in inflammatory lung disease. *Chem Biol Interact*. 2021;345:109568. doi:10.1016/j.cbi.2021.109568
55. Zhang Q, Lenardo MJ, Baltimore D. 30 Years of NF-kappaB: a blossoming of relevance to human pathobiology. *Cell*. 2017;168(1–2):37–57. doi:10.1016/j.cell.2016.12.012
56. Perkins ND. The diverse and complex roles of NF-kappaB subunits in cancer. *Nat Rev Cancer*. 2012;12(2):121–132. doi:10.1038/nrc3204
57. Christian F, Smith EL, Carmody RJ. The regulation of NF-kappaB subunits by phosphorylation. *Cells*. 2016;5(1):12. doi:10.3390/cells5010012
58. Zhang Y, Yang G, Huang S, et al. Regulation of Cr(VI)-induced premature senescence in L02 hepatocytes by ROS-Ca(2+)-NF-kappaB Signaling. *Oxid Med Cell Longev*. 2022;2022:7295224. doi:10.1155/2022/7295224

59. Bohuslav J, Chen LF, Kwon H, Mu Y, Greene WC. p53 induces NF-kappaB activation by an IkappaB kinase-independent mechanism involving phosphorylation of p65 by ribosomal S6 kinase 1. *J Biol Chem*. 2004;279(25):26115–26125. doi:10.1074/jbc.M313509200
60. Sasaki CY, Barberi TJ, Ghosh P, Longo DL. Phosphorylation of RelA/p65 on serine 536 defines an IkappaBalpha-independent NF-kappaB pathway. *J Biol Chem*. 2005;280(41):34538–34547. doi:10.1074/jbc.M504943200
61. Hochrainer K, Racchumi G, Anrather J. Site-specific phosphorylation of the p65 protein subunit mediates selective gene expression by differential NF-kappaB and RNA polymerase II promoter recruitment. *J Biol Chem*. 2013;288(1):285–293. doi:10.1074/jbc.M112.385625